

Dark Matter annihilation in Draco: new considerations of the expected gamma flux

M. A. Sánchez-Conde¹, F. Prada¹, E. L. Lokas², M. E. Gómez³, R. Wojtak² and M. Moles¹

¹ Instituto de Astrofísica de Andalucía (CSIC), E-18008, Granada, Spain

² Nicolaus Copernicus Astronomical Centre, Bartycka 18, 00-716 Warsaw, Poland

³ Departamento de Física Aplicada, Facultad de Ciencias Experimentales, Universidad de Huelva, 21071 Huelva, Spain

E-mail: masc@iaa.es

Abstract. A new revision of the gamma flux that we expect to detect in Imaging Atmospheric Cherenkov Telescopes (IACTs) from SUSY dark matter annihilation in the Draco dSph is presented using the dark matter density profiles compatible with the latest observations. This revision takes also into account the important effect of the Point Spread Function (PSF) of the telescope. We show that this effect is crucial in the way we will observe and interpret a possible signal detection. In particular, it could be impossible to discriminate between a cuspy and a cored dark matter density profile due to the fact that both density profiles may yield very similar flux profile observed by the telescope. Finally, we discuss the prospects to detect a possible gamma signal from Draco for current or planned experiments, i.e. MAGIC, GLAST and GAW.

PACS numbers: 95.35.+d; 95.55.Ka; 95.85.Pw; 98.35.Gi; 98.52.Wz

1. Introduction

Nowadays, it is generally believed that only a small fraction of the matter in the Universe is luminous. The “dark” side is supposed to be composed mostly of weakly interacting massive particles (WIMPs). Amongst all the possible particles, the most suitable candidate seems to be the lightest particle predicted by the supersymmetric extension (SUSY) of the standard model, i.e. the neutralino. At present, the indirect searches for SUSY dark matter (DM) are possible thanks to the new Imaging Atmospheric Cherenkov Telescopes (IACTs). This search is based on the detectability of gamma rays coming from the annihilation of the SUSY DM particles, that occurs in those places in the Universe where the DM density is high enough. IACTs in operation like MAGIC [1] or HESS [2], or in the near future the GLAST [3] satellite, will play a very important role in these DM searches.

A relevant question concerning the search of SUSY DM is where to search for the annihilation gamma ray signal. Due to the fact that the gamma flux is proportional to the square of the DM density, we will need to point our IACT telescope to places where we expect to find a high concentration of dark matter. In principle, the best option seems to point to the Galactic Centre (GC), since it satisfies this condition and it is also very near compared to other potential targets. However, the GC is a very

crowded region, which makes it difficult to discriminate between a possible γ -ray signal due to DM annihilation and other astrophysical sources. Whipple [4], Cangaroo [5], and specially HESS [6] and MAGIC [7] have already carried out detailed observations of the GC and all of them reported a gamma point-like source at the Sag A* location. However, if this signal was interpreted as fully due to DM annihilation, it would correspond to a very massive neutralino not compatible with the WMAP cosmology [8]. Furthermore, an extended emission was also discovered in the GC area, but it correlates very well with already known dense molecular clouds [9]. Very recently, new HESS data on the GC have been published and a reanalysis have been carried out by the HESS collaboration [10]. In this work, they especially explore the possibility that some portion of the detected signal is due to DM annihilation. According to their results, at the moment it is not possible to exclude a DM component hidden under a non-DM power-law spectrum due to an astrophysical source.

There are also other possible targets with high dark matter density in relative proximity from us, which are not plagued by the problems of the GC, e.g. the Andromeda galaxy, the dwarf spheroidal (dSph) galaxies - most of them satellites of the Milky Way- or even massive clusters of galaxies (e.g. Virgo). DSph galaxies represent a good option, since they are dark matter dominated systems with very high mass to light ratios, and at least six of them are nearer than 100 kpc from the GC (Draco, LMC, SMC, CMa, UMi and Sagittarius).

Concerning DM detection, there are two unequivocal signatures to be sure that the γ -ray signal is due to SUSY DM annihilation: the spectrum of the source, which has a very characteristic slope [8], and the spatial extension of the source, that should be extended and diffuse, but should also exhibit a characteristic shape of the flux profile. Nevertheless, we must note that if we use an instrument that does not have a resolution good enough compared to the extension of the source, we might see only a point-like source instead of a diffuse or extended one. This means that, although we might reach a sensitivity high enough for a successful detection, we would not be sure whether our signal is due to DM annihilation or not. Therefore, it is clear that it is really important to resolve the source so we can conclude that it can be interpreted as DM annihilation.

In this work, we specially focus on this last question. To do that, we first calculate the expected gamma ray flux profiles in a typical IACT due to DM annihilation in the Draco dSph, which represents a very good candidate to search for DM. Draco, located at 80 kpc, is one of the dwarfs with many observational constraints, which has helped to determine better its DM density profile. This fact is very important if we really want to make a realistic prediction of the expected γ -ray flux. These flux predictions have been already done for Draco using different models for the DM density profiles [11, 12, 13, 14]. Nevertheless, in our case, we compute these flux predictions for a cuspy and a cored DM density profiles built from the latest stellar kinematic observations together with a rigorous method of removal of interloper stars.

Once we have obtained the flux profiles, we will use them to stress the role of the Point Spread Function (PSF) of the telescope. Including the PSF, which is directly related to the angular resolution of the IACT, is essential to correctly interpret a possible signal profile due to DM annihilation. In fact, we will show that, depending on the PSF of the IACT, we could distinguish or not between different models of the DM density profile using the observed flux profile. In the case of the cuspy and cored DM density profiles that we use, it could be impossible to discriminate between them if the PSF is not good enough. It is worth mentioning that most of previous works in

the literature (except [15]) that calculated the expected flux profiles in IACTs due to dark matter annihilation did not take into account this important effect. Because of that, to emphasize the role of the PSF constitutes one of the main goals of this work.

Finally, we present the DM detection prospects for some current or planned experiments, i.e. MAGIC, GLAST and GAW. We carry out the calculations under two different approaches: detection of the gamma ray flux profile from the cusp and core DM models for Draco, and detection of an excess signal in the direction of Draco. We will show how the first approach gives us a lot of information about the origin of the gamma ray flux profile, but it is harder to have success than in the second approach, where even the PSF of the instrument is not essential and still we can extract some important conclusions.

The paper is organised as follows. In Section 2 we first present all the equations necessary to properly calculate the expected γ -ray flux in IACTs due to DM annihilation. In Section 3 we show in detail the model that we use for the DM distribution in Draco. In Section 4 we calculate the Draco flux predictions. We also stress the important role of the PSF. In Section 5, the prospects to detect signal due to DM annihilation in Draco are shown for some current or planned experiments, i.e. MAGIC, GLAST and GAW. Conclusions are finally given in Section 6.

2. The γ -ray flux in IACTs

The expected total number of continuum γ -ray photons received per unit time and per unit area in a telescope with an energy threshold E_{th} is given by the product of two expressions:

$$F(E > E_{th}) = \frac{1}{4\pi} f_{SUSY} \cdot U(\Psi_0). \quad (1)$$

where Ψ_0 represents the direction of observation relative to the centre of the dark matter halo. The factor f_{SUSY} includes all the particle physics, whereas the factor $U(\Psi_0)$ involves all the astrophysical properties (such as the dark matter distribution and geometry considerations) and also accounts for the beam smearing of the telescope.

2.1. Particle physics: the f_{SUSY} parameter

In R-parity conserving supersymmetric theories, the lightest SUSY particle (LSP) remains stable. Models predicting the lightest neutralino as the LSP are specially attractive because the lightest neutralino is a good WIMP candidate with a relic density compatible with the WMAP bounds (for a recent review see Ref. [16] and references therein).

The properties of the neutralinos are determined by its gaugino-higgsino composition:

$$\chi \equiv \chi_1^0 = N_{11}\tilde{B} + N_{12}\tilde{W}^3 + N_{13}\tilde{H}_1^0 + N_{14}\tilde{H}_2^0 \quad (2)$$

At leading order, neutralinos do not annihilate into two-body final states containing photons. However, at one loop it is possible to get processes such as [17, 18, 19]:

$$\begin{aligned} \chi + \chi &\rightarrow \gamma\gamma \\ \chi + \chi &\rightarrow Z\gamma \end{aligned}$$

with outgoing photos of energies

$$E_\gamma \sim m_\chi, \quad E_\gamma \sim m_\chi - \frac{m_Z^2}{4m_\chi} \quad (3)$$

respectively.

The relative dominance of the corresponding $v\sigma_{\gamma\gamma} \equiv v\sigma_{\chi\chi \rightarrow \gamma\gamma}$ or $v\sigma_{\chi\chi \rightarrow \gamma Z} \equiv v\sigma_{\gamma Z}$ depends on the gaugino–higgsino composition of the annihilating neutralinos.

Let us consider the mSUGRA models, where the soft terms of the MSSM are taken to be universal at the gauge unification scale M_{GUT} . Under this assumption, the effective theory at energies below M_{GUT} depends on four parameters: the soft scalar mass m_0 , the soft gaugino mass $m_{1/2}$, the soft trilinear coupling A_0 , and the ratio of the Higgs vacuum expectation values, $\tan\beta = \langle H_u^0 \rangle / \langle H_d^0 \rangle$. In addition, the minimization of the Higgs potential leaves undetermined the sign of the Higgs mass parameter μ .

To provide some specific values, we assume $A_0 = 0$, $\mu > 0$ and two values of $\tan\beta$, 10 and 50. In Fig. 1 we displayed some lines of constant values of $2v\sigma_{\gamma\gamma}$ and $v\sigma_{\gamma Z}$ on the plane $m_0 - m_{1/2}$ along with the constraints derived from the lower bound on the mass of the lightest neutral higgs, $m_h^0 = 114.1$ GeV, chargino mass $m_{\tilde{\chi}^+} = 103$ GeV and $\text{BR}(b \rightarrow s\gamma)$ and the areas with Ωh^2 on the WMAP bounds. Also we provide the lines with constant values for the elastic scattering χ –proton, relevant for neutralino direct detection.

In the computation we used DarkSUSY [20] combined with isasugra [21] implementing the phenomenological constraints as discussed in Ref. [22], the estimation of $\text{BR}(b \rightarrow s\gamma)$ was performed using Refs. [23, 24].

On the lower area consistent WMAP the neutralino is Bino–like, the relic density is satisfied mostly due to coannihilations $\chi - \tilde{\tau}$ and in the case of $\tan\beta = 50$ because of annihilations $\chi - \chi$ through resonant channels. On this sector $2v\sigma_{\gamma\gamma}$ is dominant by a factor of 10 respect $v\sigma_{\gamma Z}$, however its larger values lies on the areas constrained by the bounds on $m_{\tilde{\chi}^+}$, m_{h^0} and $\text{BR}(b \rightarrow s\gamma)$.

The higher area consistent with WMAP lies on the hyperbolic branch, the neutralino is gaugino–higgsino mixed. On this region $v\sigma_{\gamma Z}$ is larger than $2v\sigma_{\gamma\gamma}$. The position of this region is very dependent on the mass of the top, we used $m_t = 175$ GeV.

In Fig. 2 we present the values of f_{SUSY} versus the threshold energy of the detector, starting at $E_{th} = 10$ GeV, for neutralinos satisfying relic density and phenomenological constraints. f_{SUSY} is calculated as:

$$f_{SUSY} = \frac{\theta(E_{th} > m_\chi) \cdot 2v\sigma_{\gamma\gamma} + \theta(E_{th} > m_\chi - \frac{m_Z^2}{2m_\chi}) \cdot v\sigma_{\gamma Z}}{2m_\chi^2}, \quad (4)$$

where θ is the step function.

The area with higher values of f_{SUSY} correspond to points on hyperbolic branch. We can also appreciate that on the $\chi - \tilde{\tau}$ coannihilation area, m_χ has an upper bound beyond which the relic density constraint is no longer satisfied. The larger values of f_{SUSY} are not displayed since they correspond to low values of $m_{1/2}$ suppressed by the bounds on $m_{\tilde{\chi}^+}$, m_{h^0} and $b \rightarrow s\gamma$.

It is interesting to remark that the higher values of f_{SUSY} on the constrained areas lie in which the $\sigma_{\chi-p}$ reaches values in the range of direct detection experiments like Genius [25].

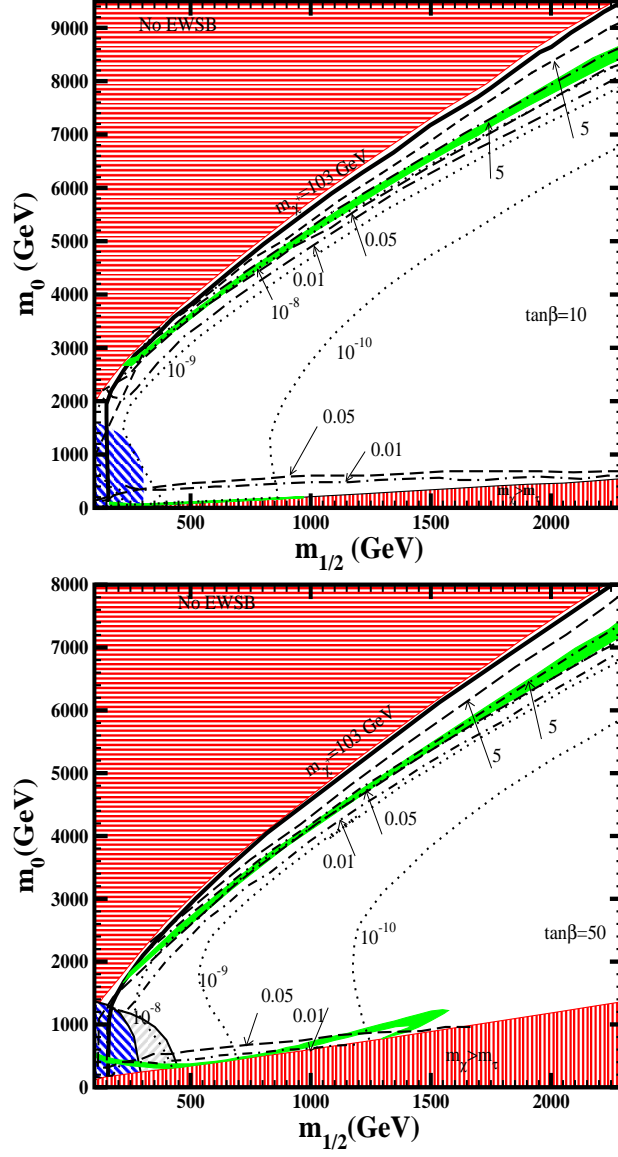


Figure 1. Contours on the $m_0 - m_{1/2}$ plane, the up and down ruled areas are excluded by the not satisfaction of the EWSB (up) and because $m_\chi > m_{\tilde{\tau}}$. The area below the upper thick solid line satisfies the experimental bound on the chargino mass, while the green shaded areas indicate the areas that predict neutralino relic density on WMAP bounds. From left to right, the ruled areas are excluded by the bounds on m_h^0 and $BR(b \rightarrow s\gamma)$ respectively. The dotted lines indicates the values of $\sigma_{\chi\bar{\chi}}$ in pb, the dash and dot-dash lines corresponds respectively to $2v\sigma_{\chi\chi \rightarrow \gamma\gamma}$ and $v\sigma_{\chi\chi \rightarrow Z\gamma}$ in units of $10^{-29} \text{cm}^3 \text{s}^{-1}$.

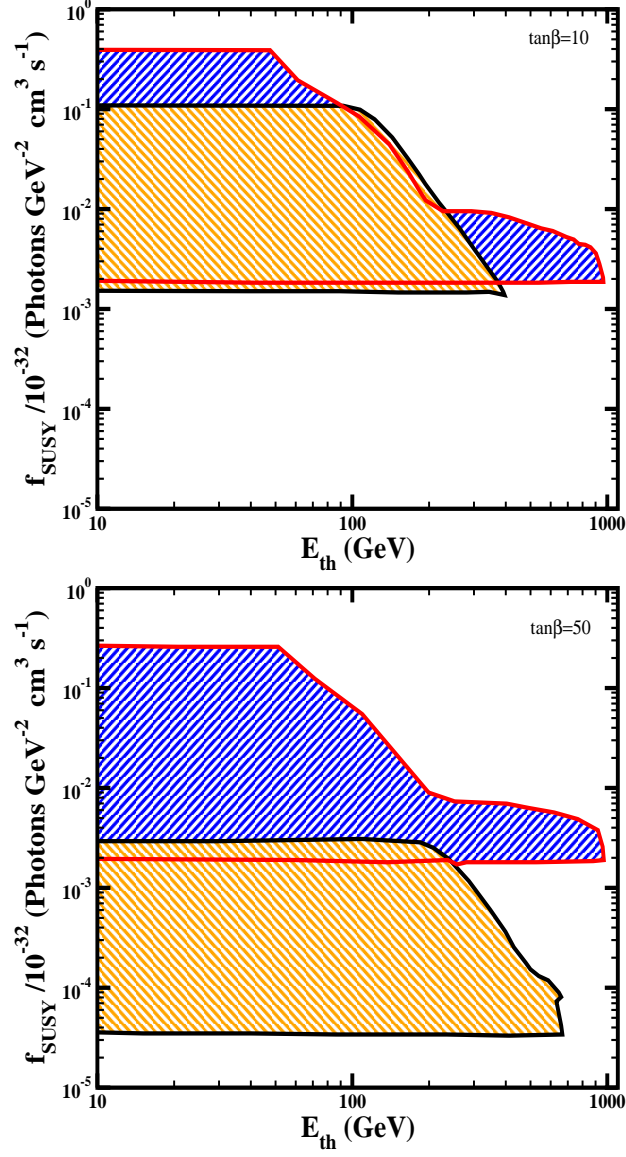


Figure 2. Values of f_{susy} as a function of E_{th} , for the points in Fig. on the WMAP region and satisfying all the phenomenological constraints. The upper (lower) region part corresponds to the upper (lower) allowed WMAP area in Fig.

2.2. Astrophysics: the $U(\Psi_0)$ parameter

All the astrophysical considerations are included in the expression $U(\Psi_0)$ in Eq.(1). This factor accounts for the dark matter distribution, the geometry of the problem and also the beam smearing of the IACT, i.e.

$$U(\Psi_0) = \int J(\Psi) B(\Omega) d\Omega \quad (5)$$

where $B(\Omega)d\Omega$ represents the beam smearing of the telescope, commonly known as the Point Spread Function (PSF). The PSF can be well approximated by a Gaussian:

$$B(\Omega)d\Omega = \exp\left[-\frac{\theta^2}{2\sigma_t^2}\right] \sin\theta \, d\theta \, d\phi \quad (6)$$

with σ_t the angular resolution of the IACT. The PSF plays a very important role in the way we will observe a possible DM signal in the telescope. However, most of previous works in the literature did not take into account its effect (except [15]; in [26] the PSF apparently was also used, although it is not mentioned in the text (S. Profumo, private communication)). In Section 4 we will study in detail the importance of the PSF in the determination of the gamma ray flux profile.

The $J(\Psi)$ factor of Eq.(5) represents the integral of the line-of-sight of the square of the dark matter density along the direction of observation Ψ :

$$J(\Psi) = \int_{l.o.s.} \rho_{dm}^2(r) \, d\lambda = \int_{\lambda_{min}}^{\lambda_{max}} \rho_{dm}^2[r(\lambda)] \, d\lambda \quad (7)$$

Here, r represents the galactocentric distance, related to the distance λ to the Earth by:

$$r = \sqrt{\lambda^2 + R_\odot^2 - 2 \lambda R_\odot \cos \Psi} \quad (8)$$

where R_\odot is the distance from the Earth to the centre of the galactic halo, and Ψ is related to the angles θ and ϕ by the relation $\cos \Psi = \cos \psi_0 \cos \theta + \sin \psi_0 \sin \theta \cos \phi$. The lower and upper limits λ_{min} and λ_{max} in the l.o.s. integration are given by $R_\odot \cos \psi \pm \sqrt{r_t^2 - R_\odot^2 \sin^2 \psi}$, where r_t is the tidal radius of the dSph galaxy in this case..

3. Dark matter distribution in Draco

In our modelling of Draco we used the sample of 207 Draco stars with measured line-of-sight velocities originally considered as members by [27]. In selecting these stars these authors relied on a simple prescription going back to [28] and based on rejection of stars with velocities exceeding $3\sigma_{los}$ where σ_{los} is the line-of-sight velocity dispersion of the sample. [29] have shown that if all these 207 stars are used to model Draco velocity distribution the resulting velocity moments can be reproduced only by extremely extended mass distribution with total mass of the order of a normal galaxy. Their arguments strongly suggested that some of the stars may in fact be unbound and the simple $3\sigma_{los}$ rejection of stars is insufficient.

Here we apply a rigorous method of removal of such interlopers originally proposed by [30] and applied to galaxy clusters. The method relies on calculating the maximum velocity available to the members of the object assuming that they are on circular orbits or infalling into the structure. The method was shown to be the most efficient among many methods of interloper removal recently tested on cluster-size simulated dark matter haloes by [31]. Its applicability and efficiency in the case of dSph galaxies was demonstrated by [32]. Fig. 3 shows the results of the application of this procedure to Draco. The 207 stars shown in the plot are divided into those iteratively rejected by the procedure (open circles) and those accepted at the final iteration (filled circles).

The final sample with 194 stars is different from any of the three considered by [29] therefore we repeat their analysis here for this new selection. Our analysis is exactly

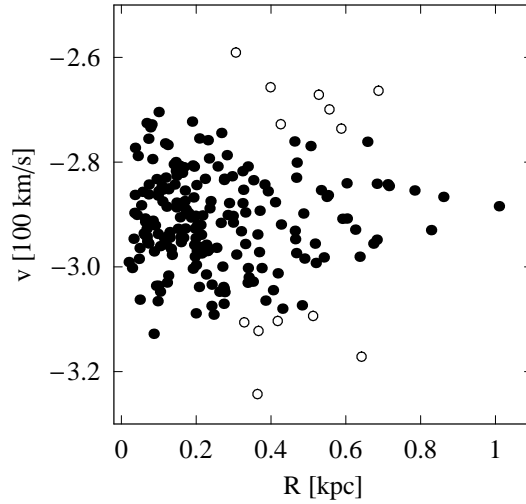


Figure 3. The line-of-sight velocities versus projected distances from the galaxy centre for 207 stars from [27]. Open circles mark the 13 stars rejected by our interloper removal procedure, filled circles show the 194 ones accepted.

the same, except that in the calculation of the velocity moments we use 32-33 stars per bin instead of about 40 and we consider a DM profile with a core in addition to the cuspy one. The profiles of the line-of-sight velocity moments, dispersion and kurtosis, obtained for the new sample are shown in Fig. 4. The kurtosis was expressed in terms of the variable $k = [\log(3K/2.7)]^{1/10}$ where K is the standard kurtosis estimator. We assumed that the DM distribution in Draco can be approximated by

$$\rho_d(r) = Cr^{-\alpha} \exp\left(-\frac{r}{r_b}\right) \quad (9)$$

proposed by [33], which was found to fit the density distribution of a simulated dwarf dark matter halo stripped during its evolution in the potential of a giant galaxy. In the same work it was found that the halo, which initially had a NFW distribution, preserves the cusp in the inner part (so that $\alpha = 1$ fits the final remnant very well) but develops an exponential cut-off in the outer parts. Here we will consider two cases, the profile with a cusp $\alpha = 1$ and a core $\alpha = 0$. It remains to be investigated which scenarios could lead to such core profiles.

The best-fitting solutions to the Jeans equations (see [29]) for two component models with dark matter profiles given by (9) are plotted in Fig. 4 as solid lines in the case of the cuspy profile and dashed lines for the core. The best-fitting parameters of the two models are listed in Table 1, where M_D/M_S is the ratio of the total dark matter mass to total stellar mass, r_b/R_S is the break radius of equation (9) in units of the Sérsic radius of the stars and β is the anisotropy parameter of the stellar orbits.

Fig. 5 shows the best-fitting dark matter density profiles in the case of the cusp (solid line) and the core (dashed line). As we can see, both density profiles are similar up to about 1 kpc, where they are constrained by the data. The reason for very different values of the break radius r_b in both cases is the following. The kurtosis is sensitive mainly to anisotropy and it forces β to be close to zero in both cases. However, to reproduce the velocity dispersion profile with $\beta \approx 0$ the density profile

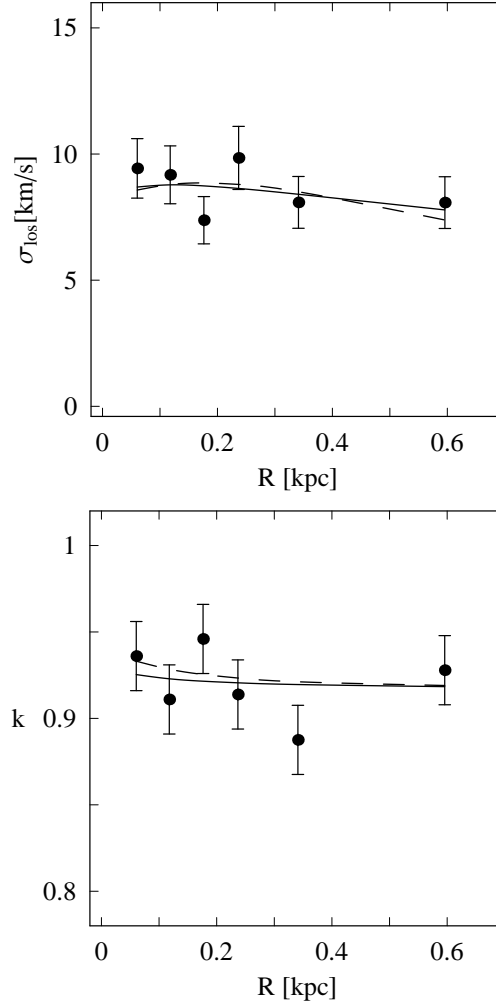


Figure 4. The line-of-sight velocity dispersion (upper panel) and kurtosis variable k (lower panel) calculated for the sample of 194 stars with 32-33 stars per bin. The lines show the best-fitting solutions of the Jeans equations for the DM profile with a cusp (solid lines) and a core (dashed lines).

Table 1. Best-fitting parameters of the two-component models for the DM profiles with a cusp ($\alpha = 1$) and a core ($\alpha = 0$) obtained from joint fitting of velocity dispersion and kurtosis profiles shown in Fig. 4. The last column gives the goodness of fit measure χ^2/N .

profile	M_D/M_S	r_b/R_S	β	χ^2/N
cusp	830	7.0	-0.1	8.8/9
core	185	1.4	0.06	9.5/9

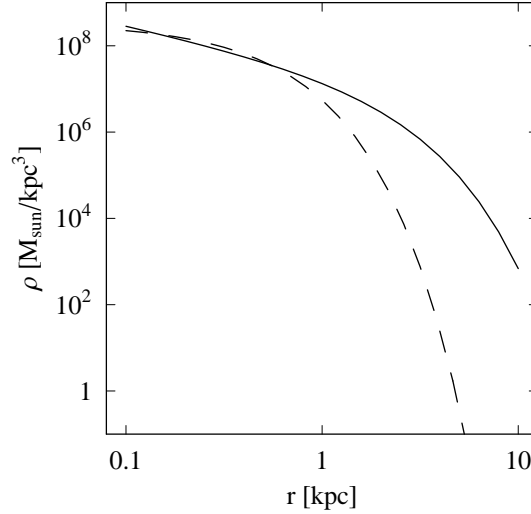


Figure 5. The best-fitting DM density profiles for Draco with a cusp (solid line) and a core (dashed line).

Table 2. Values of C and r_b for a cuspy and a cored DM density profile given by Eq.(9), as deduced from those parameters listed in Table 1.

profile	C	r_b (kpc)
cuspy	$3.1 \times 10^7 \text{ M}_\odot/\text{kpc}^2$	1.189
core	$3.6 \times 10^8 \text{ M}_\odot/\text{kpc}^3$	0.238

has to be steep enough. In the case of the core it means that the exponential cut-off has to occur for rather low radii, which is what we see in the fit. The cuspy profile does not need to steepen the profile so much so it is much more extended and its total mass is much larger.

4. Draco gamma ray flux profiles

In order to compute the expected gamma flux, we need to calculate the value of the “astrophysical factor”, $U(\psi_0)$, given in Eq.(1) and presented in detail in Section 2.2. We calculated it for the cored ($\alpha = 0$) and cuspy ($\alpha = 1$) density profiles given by Eq.(9) using the parameters listed in Table 2 (that were deduced from those given in Table 1 and where we used $R_S = 7.3$ arcmin for Draco, following [34]). R_\odot was set to 80 kpc, as derived from an analysis on the basis of wide-field CCD photometry of resolved stars in Draco [35]. For the tidal radius we used a value of 7 kpc as given by [12] and derived from the Roche criterion supposing an isothermal profile for the Milky Way. Nevertheless, this value depends strongly on the profile used for the Milky Way and Draco, e.g. a value of 1.6 kpc is found when a NFW DM density profile is used for both galaxies. It is worth mentioning, however, that the calculation of $J(\Psi)$ depends weakly on r_t and we could have chosen another value $r_t \gtrsim 1$ kpc.

There is another issue that we will have to take into account in order to calculate

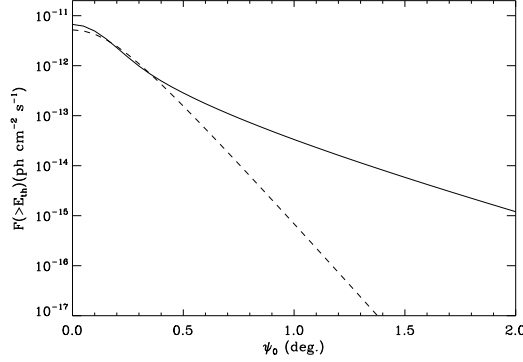


Figure 6. Draco flux predictions for the cored (dashed line) and cuspy (solid line) density profiles, computed using a PSF= 0.1°.

$U(\psi_0)$. If we integrate the square DM density along the line of sight using a cuspy DM density profile, we will obtain divergences at angles $\psi_0 \rightarrow 0$ (clearly there will not be any problem for core profiles). This can be solved by introducing a small constant DM core in the very centre of the DM halo. In particular, the radius r_{cut} at which the self annihilation rate $t_l \sim (\langle \sigma_{ann} v \rangle n_\chi r_{cut})^{-1}$ equals the dynamical time of the halo $t_{dyn} \sim (G \bar{\rho})^{-1/2}$, where $\bar{\rho}$ is the mean halo density and n_χ is the neutralino number density, is usually taken as the radius of this constant density core [36]. For the NFW DM density profile this value for r_{cut} is of the order of $10^{-13} - 10^{-14}$ kpc. For steeper DM density profiles (such as the compressed NFW or the Moore profile) a value of $r_{cut} \sim 10^{-8}$ kpc is obtained. We used a value of 10^{-8} kpc in all our computations. We must note that r_{cut} represents a lower limit concerning the acceptable values for this parameter, so the obtained fluxes should be taken as upper bounds.

Once we have calculated $U(\psi_0)$, we will need also to take a value for the f_{SUSY} parameter in order to obtain the absolute flux due to DM annihilation (see Eq. 1). We chose a value of $f_{SUSY} = 10^{-33} \text{ ph GeV}^{-2} \text{ cm}^3 \text{ s}^{-1}$ in all our computations for a typical $E_{th} \sim 100$ GeV of the IACT. This value corresponds to the most optimistic value possible to adopt for f_{SUSY} according to Fig. 2 for the two different values of $\tan \beta$ presented.

The resulting γ -ray flux profiles for Draco are plotted in Figure 6, where we used a PSF with $\sigma_t = 0.1^\circ$ (to simplify the notation, hereafter we will use PSF= 0.1° to refer to a PSF with $\sigma_t = 0.1^\circ$). This value of 0.1° is the typical value for an IACT like MAGIC or HESS. As we can see, it could be possible to distinguish between a cored and a cuspy density profile thanks to a different and characteristic shape of the flux profile in each case.

To illustrate the PSF effect on the shape of the observed flux profile with IACTs, in the top panel of Figure 7 we show the same as in Fig. 6, but here for a PSF= 1°. It is clear that, although we use different DM density profiles, a worse telescope resolution makes both resulting flux profiles for a core and a cusp indistinguishable. We may think that we could distinguish them from the value of the absolute flux. However, the difference in the absolute flux between both DM density profiles is very small and in practice the distinction would be impossible. Moreover, there are many uncertainties in this absolute flux coming from the particle physics. f_{SUSY} may be very different from the most optimistic case assumed here, since it could vary more than three orders

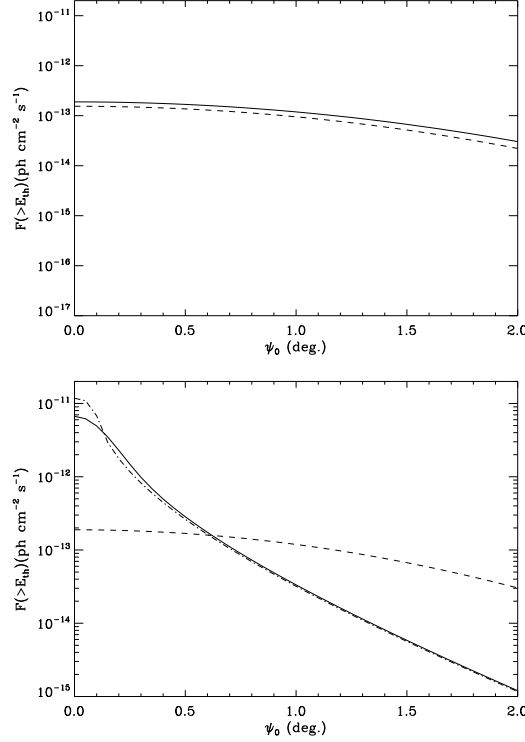


Figure 7. Top panel: Draco flux predictions for the cored (dashed line) and cuspy (solid line) density profiles, computed using a PSF= 1° . Bottom panel: Draco flux predictions for the cuspy density profile using two different PSFs. Solid line corresponds to PSF= 0.1° and dashed line to PSF= 1° . The flux profile computing without PSF is also shown for comparison (dot-dashed line).

of magnitude for this SUSY model (see Fig. 2). The uncertainty due to the DM density profile to be core or cusp is negligible at least in the inner 0.5 degrees.

Concerning the effect of the PSF given the same DM density profile, a worse telescope resolution flattens the flux profile. It can be clearly seen in the bottom panel of Figure 7, where we plot the Draco γ -ray flux predictions only for the cuspy density profile but using two different values of the PSF (0.1° and 1°), and where we plot also the same flux profile computed without PSF for comparison.

A good example to show the real importance of the telescope resolution can be found in the controversy generated in the wake of the Draco γ -ray excess reported by the CACTUS collaboration in 2005 [37]. Now, it seems clear that this excess was probably due to a poor understanding of the background, i.e. to the difficulties in separating hadrons from gamma photons in such experiment, not optimised for γ -ray astronomy (in fact, the PSF of this experiment is very poor, around 1°). However, concerning our line of work and always with the intention of clarifying the role of the PSF, we must mention the results shown in [26]. There, the CACTUS data were superimposed on different flux profiles (each of them related to possible models of DM density profiles for Draco) in Figure 2. As mentioned before, the CACTUS PSF is around 1° , whereas the different flux profiles superimposed for comparison to the

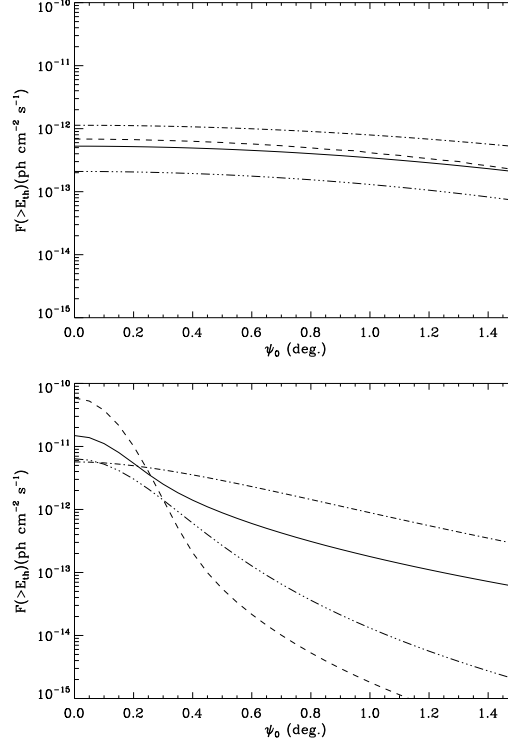


Figure 8. Draco flux profiles for the four models of DM density profile used in [26] (NFW1 (solid line); NFW2 (dashed line); BUR1 (dot-dashed line); BUR2 (3dots-dashed line)), computed using the CACTUS PSF= 1° (top panel), and using an improved PSF= 0.1° (bottom panel).

CACTUS data were computed using an angular resolution of 0.1° . Looking at that figure, one may come to the conclusion that a cored profile seems to be the most adequate DM density profile for Draco, as opposed to the cuspy profile.

However, it would be more appropriate to make the comparison between the CACTUS data and the flux profiles using in both cases the same PSF of the experiment. Doing so, we will now obtain the results shown in the top panel of Figure 8. As we can see, if we properly take into account the PSF effect, it would be impossible to use the CACTUS data to discriminate between different flux profiles, i.e. between the four models for the density profile described in [26], since all of these flux profiles have essentially the same shape. Only the absolute flux could give us a clue to make the distinction possible, but as mentioned before there are too many uncertainties in the y-axis to extract solid conclusions. In the bottom panel of Figure 8 the same exercise was done, but now taking an improved PSF= 0.1° (e.g. the MAGIC PSF). In this case we can see that it could be possible to distinguish between different flux profiles (although first we would need to check if our IACT reaches a sensitivity good enough to observe an extended profile).

5. Detection prospects for some current or planned experiments

Due to some misunderstanding in the computation of the fluxes, this section is now being revised. We will replace this current version of the paper as soon as possible to include the correct flux profiles as well as the appropriate calculations concerning the signal excess detection.

5.1. Flux profile detection

5.2. Excess signal detection

6. Conclusions

In this work we focused on the possibility to detect a signal coming from SUSY DM annihilation in the Draco dwarf. This galaxy, a satellite of the Milky Way, represents one of the best suitable candidates to search for dark matter outside our galaxy, since it is near and it has probably more observational constraints than any other known dark matter dominated system. This fact becomes crucial when we want to make realistic predictions of the expected observed γ -ray flux due to DM annihilation.

Draco is a dwarf galaxy tidally stripped by the Milky Way, so it seems preferable to build a model for the mass distribution that takes into account this important fact. Using this more appropriate model for Draco, we have obtained the γ -ray flux profiles for the case of a cuspy and a cored DM density profiles (both scenarios are equally valid according to the observations). To do that, we first estimated the best-fitting parameters for each density profile by adjusting the solutions of the Jeans equations to velocity moments obtained for the Draco stellar sample cleaned by a rigorous method of interloper removal. For both cuspy and cored DM density profiles, the flux values that we obtain are very similar for the inner region of the dwarf, i.e. where we have the largest flux values and signal detection would be easier.

There is, however, a way to distinguish between a cored and a cuspy DM density profile. The crucial points concerning this issue are the sensitivity and the PSF of the telescope. If the telescope resolution is good enough (and we reach the required sensitivity) a distinction between both cusp and core models may be possible thanks to the shape of the flux profile in each case. However, if the PSF of the instrument is poor, its effect could make it impossible to discriminate between different flux profiles, i.e. different models of the DM density profile. In any case, to be sure at least that the signal is due to DM annihilation, we will need to have a PSF good enough to be able to resolve the source, i.e. we will need to detect with a good resolution at least a portion of the flux profile large enough so we can conclude that it belongs to DM annihilation.

Finally, it is worth mentioning that IACTs that join a large field of view with a high sensitivity will be necessarily the future in this field and will provide a next step in DM searches. GAW, a R&D experiment under development with an energy threshold ~ 700 GeV and a $24^\circ \times 24^\circ$ field of view, constitutes a first attempt in this direction.

Acknowledgments

M.A.S.C. acknowledges the support of an I3P-CSIC fellowship in Granada. M.A.S.C. and F.P. also acknowledge the support of the Spanish AYA2005-07789 grant. E.L.L.

and R.W. are grateful for the hospitality of the Instituto de Astrofísica de Andalucía during their visit. This work was partially supported by the Polish Ministry of Science and Higher Education under grant 1P03D02726 and the Polish-Spanish exchange program of CSIC/PAN. M.E.G. acknowledges support from the 'Consejería de Educación de la Junta de Andalucía', the Spanish DGICYT under contracts BFM2003-01266, FPA2006-13825 and European Network for Theoretical Astroparticle Physics (ENTApP), member of ILIAS, EC contract number RII-CT-2004-506222.

References

- [1] Lorentz E. *et al* , 2004, *New Astron. Rev.*, **48**, 339
- [2] Hinton J. A., 2004, *New Astron. Rev.*, **48**, 331
- [3] Gehrels N. and Michelson P., 1999, *Astropart. Phys.*, **11**, 277
- [4] Kosack K. *et al* , 2004, *ApJ*, **608**, L97
- [5] Tsuchiya K. *et al* , 2004, *ApJ*, **606**, L115
- [6] Aharonian F. *et al* , 2004, *A&A*, **425**, L13
- [7] Albert J. *et al* , 2006, *ApJ*, **638**, L101
- [8] Bergstrom L. *et al* , 2005, *Phys. Rev. Lett.*, **95**, 241301
- [9] Aharonian F. *et al* , 2006, *Nature*, **439**, 695
- [10] Aharonian F. *et al* , 2006, *preprint*, astro-ph/0610509
- [11] Bergstrom L. and Hooper D., 2006, *Physical Review D*, **73**, 063510
- [12] Evans N. W., Ferrer F. and Sarkar S., 2004, *Physical Review D*, **69**, 123501
- [13] Colafrancesco S., Profumo S. and Ullio P., 2006, submitted to *Phys. Rev. D*, *preprint*, astro-ph/0607073
- [14] Mambrini Y., Munoz C., Nezri E. and Prada F., 2006, *JCAP*, **01**, 010
- [15] Prada F., Klypin A., Flix J., Martínez M. and Simonneau E., 2004, *Phys. Rev. Letters*, **93**, 241301
- [16] Munoz C., 2004, *Int. J. Mod. Phys. A*, **19**, 3093
- [17] Bergstrom L. and Ullio P., 1997, *Nucl. Phys. B* **504** 27
- [18] Bern Z., Gondolo P. and Perelstein M., 1997, *Phys. Lett. B* **411** 86
- [19] Ullio P. and Bergstrom L., 1998, *Phys. Rev. D*, **57**, 1962
- [20] Gondolo P., Edsjo J., Ullio P., Bergstrom L., Schelke M. and Baltz E. A., 2004, *JCAP*, **0407**, 008
- [21] Paige F. E., Protopopescu S. D., Baer H. and Tata X., 2003, *preprint*, hep-ph/0312045.
- [22] Gomez M. E., Ibrahim T., Nath P. and Skadhauge S., 2005, *Phys. Rev. D*, **72**, 095008
- [23] Belanger G., Boudjema F., Pukhov A. and Semenov A., 2006, *Comput. Phys. Commun.*, **174**, 577 and *Comput. Phys. Commun.*, 2002, **149**, 103
- [24] Gomez M. E., Ibrahim T., Nath P. and Skadhauge S., 2006, *Phys. Rev. D*, **74**, 015015
- [25] Cerdeno D. G., Gabrielli E., Gomez M. E. and Munoz C., 2003, *JHEP*, **0306**, 030
- [26] Profumo S. and Kamionkowski M., 2006, *JCAP*, **3**, 3
- [27] Wilkinson M. I., Kleya J. T., Evans N. W., Gilmore G. F., Irwin M. J. and Grebel E. K., 2004, *ApJ*, **611**, L21
- [28] Yahil A. and Vidal N. V., 1977, *ApJ*, **214**, 347
- [29] Lokas E. L., Mamon G. A. and Prada F., 2005, *MNRAS*, **363**, 918
- [30] den Hartog R. and Katgert P., 1996, *MNRAS*, **279**, 349
- [31] Wojtak R., Lokas E. L., Mamon G. A., Gottlöber S., Prada F. and Moles M., 2006, *preprint*, astro-ph/0606579
- [32] Klimontowski J., Lokas E. L., Kazantzidis S., Prada F., Mayer L. and Mamon G. A., 2006, submitted to *MNRAS*, *preprint*, astro-ph/0611296
- [33] Kazantzidis S., Mayer L., Mastropietro C., Diemand J., Stadel J. and Moore B., 2004, *ApJ*, **608**, 663
- [34] Odenkirchen M., *et al* , 2001, *AJ*, **122**, 2538
- [35] Aparicio A., Carrera R. and Martinez-Delgado D., 2001, *AJ*, **122**, 2524
- [36] Fornengo N., Pieri L. and Scopel S., 2004, *Physical Review D*, **70**, 103529
- [37] Marleau P., *TAUP*, September 2005, Zaragoza (Spain); Tripathi M., *Cosmic Rays to Colliders 2005*, Prague (Czech Republic), September 2005; *TeV Particle Astrophysics Workshop*, Batavia (USA), July 2005; Chertok M., *Proc. of Panic 05*, Santa Fe (USA), October 2005
- [38] Weekes T. C. *et al* , 2002, *Astropart. Phys.*, **17**, 221

*Dark Matter annihilation in Draco: new considerations of the expected gamma flux*¹⁶

[39] Maccarone M. C. *et al* , 2005, *Proc. of the 29th International Cosmic Ray Conference, ICRC*, **5**, 295

